Local leakage current behaviours of $BiFeO_3$ films

2011 Chinese Phys. B 20 117701

(http://iopscience.iop.org/1674-1056/20/11/117701)

Local leakage current behaviours of $BiFeO_3$ films*

Zou Cheng(邹 成)[a)b)c)], Chen Bin(陈 斌)[b)c)†], Zhu Xiao-Jian(朱小健)[b)c)], Zuo Zheng-Hu(左正笏)[b)c)], Liu Yi-Wei(刘宜伟)[b)c)], Chen Yuan-Fu(陈远富)[a)], Zhan Qing-Feng(詹清峰)[b)c)], and Li Run-Wei(李润伟)[b)c)]

[a)] *State Key Laboratory of Electronic Thin Films and Integrated Devices, University of Electronic Science and Technology of China, Chengdu* 610054, *China*

[b)] *Key Laboratory of Magnetic Materials and Devices, Ningbo Institute of Material Technology and Engineering, Chinese Academy of Sciences, Ningbo* 315201, *China*

[c)] *Zhejiang Province Key Laboratory of Magnetic Materials and Application Technology, Ningbo Institute of Material Technology and Engineering, Chinese Academy of Sciences, Ningbo* 315201, *China*

(Received 7 June 2011; revised manuscript received 19 June 2011)

The leakage current behaviours of polycrystalline $BiFeO_3$ thin films are investigated by using both conductive atomic force microscopy and current–voltage characteristic measurements. The local charge transport pathways are found to be located mainly at the grain boundaries of the films. The leakage current density can be tuned by changing the post-annealing temperature, the annealing time, the bias voltage and the light illumination, which can be used to improve the performances of the ferroelectric devices based on the $BiFeO_3$ films. A possible leakage mechanism is proposed to interpret the charge transports in the polycrystalline $BiFeO_3$ films.

Keywords: polycrystalline $BiFeO_3$ thin films, local leakage current, conductive atomic force microscopy

PACS: 77.55.Nv, 73.50.Pz, 73.50.–h **DOI:** 10.1088/1674-1056/20/11/117701

1. Introduction

Due to their combined ferroelectric and ferromagnetic properties, multiferroic materials have received great attention for applications in the high density information storage, the multifunctional magnetoelectrical sensors, etc.[1,2] Among various multiferroic materials, $BiFeO_3$ (BFO) is the most promising candidate due to its high ferroelectric and magnetic ordering temperatures (ferroelectric Curie temperature ∼1103 K and Néel temperature ∼ 640 K).[3,4] However, BFO thin films exhibit a relatively high leakage current density, which restricts their possible applications. It has been reported that small quantities of Fe^{2+} ions and oxygen vacancies in the BFO are responsible for the high leakage current.[5,6] Various efforts have been made to reduce the leakage current, and the doping with transition metal ions, such as Mn^{3+}, Cr^{2+}, and Co^{2+}, at the A site of the perovskite (ABO_3) structured BFO lattice are found to be an effective way.[7−9] In addition, various buffer layers, such as $BaSrTiO_3$ and $La_{0.8}Sr_{0.2}MnO_3$,[10,11] inserted into the electrode/BFO interface can effectively reduce the leakage current.

Prior to effectively reduce and control the leakage current in the multiferroic material, the leakage mechanism needs to be known. The effects of temperature, electrode, and thickness on the leakage current of the BFO film have been studied in detail. Pabst *et al.*[12] reported that the Poole–Frenkel (PF) emission was dominant for a high-quality epitaxial BFO film. Yang *et al.*[13] found that the leakage mechanism in Pt/BFO/$SrRuO_3$ strongly depended on the temperature and the voltage polarity. Although many efforts have been made to reduce the leakage current and to understand the leakage mechanism in the BFO film, the microscopic leakage behaviours as well as the mechanism are still not clear due to the complicated charge transport pathways, such as the grain interior,[14−16] the grain boundary,[17,18], and even the domain wall.[19] In this paper, we investigate local leakage current behaviours of a polycrystalline BFO (poly-BFO) film in a microscopic way. The local charge transport pathway imaged by using the con-

*Project supported by the Chinese Academy of Sciences, the State Key Project of Fundamental Research of China, and the Natural Science Foundation of Ningbo, China.

†Corresponding author. E-mail: chenbin@nimte.ac.cn

ductive atomic force microscopy (CAFM) is found to be related to the film fabrication process and the device working parameters. Our study provides an effective way to manipulate the conduction behaviour and pushes forward the understanding of the leakage mechanism in the poly-BFO film.

2. Experiment

Poly-BFO thin films were deposited onto commercial Pt/Ti/SiO_2/Si substrates by using the chemical solution deposition. Bismuth nitrate ($Bi(NO_3)_3{\cdot}H_2O$) and iron nitrate ($Fe(NO_3)_3{\cdot}9H_2O$) were used as the starting materials. In order to compensate the expected Bi loss during the post-annealing treatment, an excess of 2 mol% bismuth nitrate was added. The poly-BFO thin films were deposited by spin coating with the BFO solution at a speed of 5000 rpm for 10 s, and followed by preheating at 300 °C for 10 min on a hot plate in air. These processes were repeated six times to obtain a desired thickness of about 250 nm. Furthermore, different annealing processes were used to obtain various phase structures. The crystal structures and the topographies of the films were checked by the X-ray diffraction (XRD) and the atomic force microscopy (AFM), respectively. The 100 μm diameter copper top electrode pads with a thickness of 200 nm were deposited on the tops of the poly-BFO films by using the electron-beam evaporation. The current–voltage characteristics were measured using Keithley 4200 semiconductor characterization systems. The local conductance was mapped by using a conductive atomic force microscope (Dimension V, Veeco) equipped with a conductive cantilever. The bottom electrode (Pt layer) was electrically connected to a metal sample stage with a conductive tape.

3. Results and discussion

Figure 1 shows the XRD patterns for the poly-BFO films annealed at various temperatures for 10 min. No distinct peak is observed with the annealing temperature below 450 °C, indicating that the as-deposited film is amorphous. As the annealing temperature increases, the diffraction peaks of the BFO perovskite phase are observed, suggesting that the BFO films start to crystallize. The intensity of the BFO peak is increased with the increase of the annealing temperature, indicating the improvement on the crystallinity.

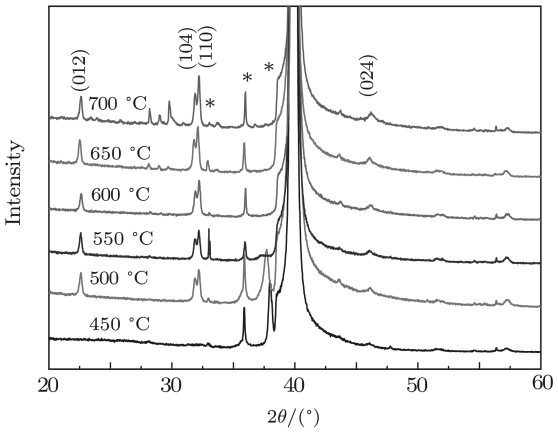

Fig. 1. XRD patterns of poly-BFO thin films prepared on Pt/TiO_2/SiO_2/Si substrates and annealed at various temperatures. The peaks of substrate are marked with stars.

The morphologies and the local current distributions of the poly-BFO films annealed in various processes were studied by means of the CAFM. Figure 2 shows the AFM and the corresponding CAFM images for the poly-BFO films annealed at various temperatures for 10 min under a constant bias voltage of 500 mV. The scanning size is 1.0 μm×1.0 μm. The AFM images show that with the increase of the annealing temperature, the grain sizes of the poly-BFO films grow up. The local charge transport pathways of the poly-BFO films simultaneously obtained by the CAFM are mostly located at the grain boundaries, while the grain interior exhibits the insulating behaviour, as marked in Fig. 2. For the annealing temperature lower than 650 °C, no charge transport pathway is observed at the bias voltage of 500 mV. With the increase of the annealing temperature, the number of the charge transport pathways increases. Furthermore, the effect of the annealing time on the local leakage current behaviour of the poly-BFO film was also studied. The annealing time ranged from 1 min to 10 min, while the annealing temperature was fixed at 650 °C. The CAFM images show that no charge transport pathway is formed until the annealing time increases up to 10 min.

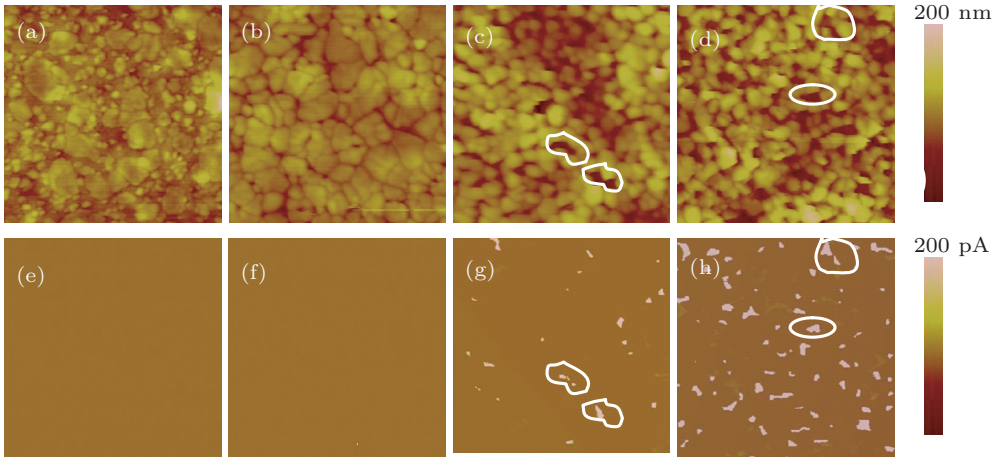

Fig. 2. (colour online) Topography images ((a)–(d)) and the corresponding CAFM images ((e)–(h)) of poly-BFO films under a bias voltage of 500 mV. The films are annealed for 10 min at temperatures of 450 °C ((a)and(e)), 550 °C ((b) and (f)), 650 °C ((c) and (g)), and 700 °C ((d) and (h)). The scanning area is 1 μm^2.

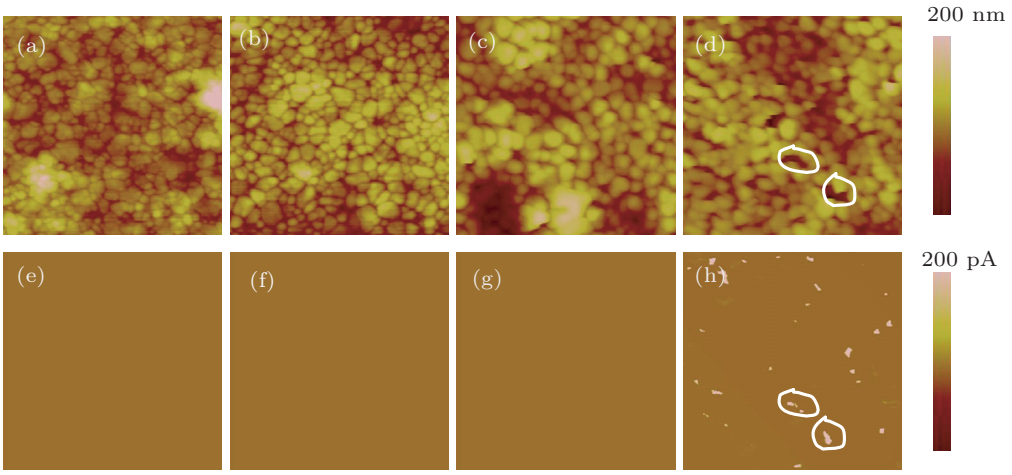

Fig. 3. (colour online) Topography images ((a)–(d)) and the corresponding CAFM images ((e)–(h)) of poly-BFO films under a bias voltage of 500 mV. The films are annealed at 650 °C for times of 1 min ((a) and (e)), 2 min ((b) and (f)), 5 min ((c) and (g)), and 10 min ((d) and (h)). The scanning area is 1 μm^2.

Based on the results shown in Figs. 2 and 3, we conclude that the amorphous phase and the small grain are helpful to reduce the leakage current in the poly-BFO films. Similar grain size dependent leakage currents have been observed in $Pb(Zr,Ti)O_3$ and $BiFeO_3$–$BiCrO_3$ films,[20,21] the leakage current density is low for the small-grain film as observed in the poly-BFO films. According to the grain boundary limited conduction theory,[22] the low leakage current density for the small-grain film is due to the inter-grain depletion layers formed at the grain boundaries. The local space charge near the grain boundaries inhibits the current flow. Consequently, the overlapped depletion regions of the neighboring grain boundaries give rise to the low leakage current. While in the large-grain film, the depletion regions of the neighboring grain boundaries cannot overlap, which provide the pathways for the charge transport and result in the high leakage current.

Since no charge transport pathway is observed in the amorphous sample, this suggests that the amorphous phase can act as a barrier layer to hinder the charge transport. The existence of the amorphous phase in the crystalline matrix and its content ratio seem to be responsible for the observed annealing parameter dependence of the local charge transport behaviour in the poly-BFO film. Therefore, it is expected that the charge transport can be modulated by precisely controlling the amorphous phase. In order to check the above scenario, two types of samples, amorphous-BFO/5-poly-BFO and poly-BFO films, were prepared, and their current behaviours

were measured. For the poly-BFO sample, all the six BFO layers were annealed at 650 °C for 10 min. For the amorphous-BFO/5-poly-BFO sample, the first five layers were annealed at 650 °C for 10 min, the sixth layer was preheated only at 300 °C for 10 min. Without any further annealing process, the sixth BFO layer remained in the amorphous phase and acted as a buffer layer. The current–voltage characteristics indicate that the leakage current density of the amorphous-BFO/5-poly-BFO film is reduced by two orders of magnitude as compared with that of the poly-BFO film, as revealed in Fig. 4. This result proves that the amorphous BFO layer is a good barrier to hinder the charge transport and reduce the leakage current.

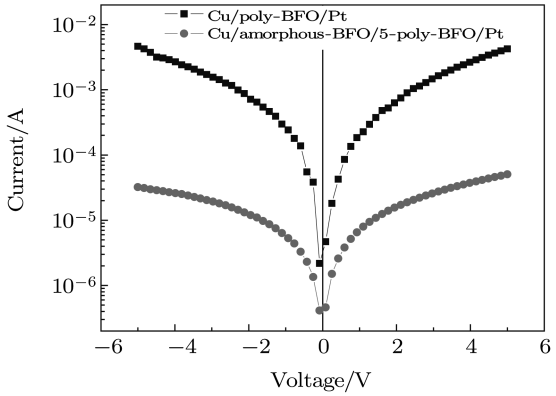

Fig. 4. Current–voltage characteristics for Cu/poly-BFO/Pt and Cu/ amorphous-BFO/5-poly-BFO /Pt capacitors.

Besides the effect of the annealing processes, we also investigated the charge transports of the poly-BFO films operated at different bias voltages and under different conditions of light illumination. Figure 5 shows a series of topography images and the corresponding CAFM images at bias voltages ranging from 10 mV to 1000 mV for the poly-BFO films. The CAFM images show that under a small bias voltage of 10 mV, a few charge transport pathways are formed. As the bias voltage increases, both the charge transport pathways and the local current intensities increase, leading to the nonlinear current–voltage characteristics in the poly-BFO films. This scenario has also been confirmed by the experimental macroscopic transport measurement.[23]

Photovoltaic effects have been observed in the BFO in both single crystal and epitaxial film forms.[24–26] Here, we measure the effect of light illumination on the leakage current of the poly-BFO film. Figure 6 shows the photo-induced local charge transports of the poly-BFO films measured by the CAFM. Under light illumination, more charge transport pathways are generated than that in the dark. This enhanced photocurrent is likely to result from the light-induced carriers in the poly-BFO film. Since it is universally believed that the photovoltaic effect in the ferroelectric material is related to the light-induced carriers and their separation under an electric field.[27,28]

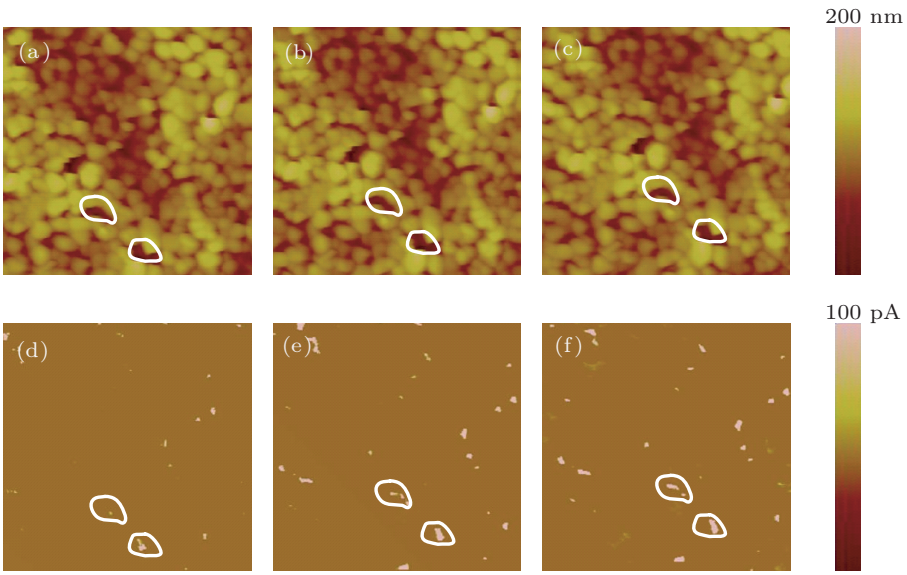

Fig. 5. (colour online) Topography images ((a)–(c)) and the corresponding CAFM current images ((d)–(f)) of a poly-BFO film annealed 650 ° for 10 min sequentially gathered from the same location at bias voltages of 10 mV ((a) and (d)), 100 mV((b) and (e)), and 1000 mV ((c) and (f)). The shown scanning area is 1 μm^2.

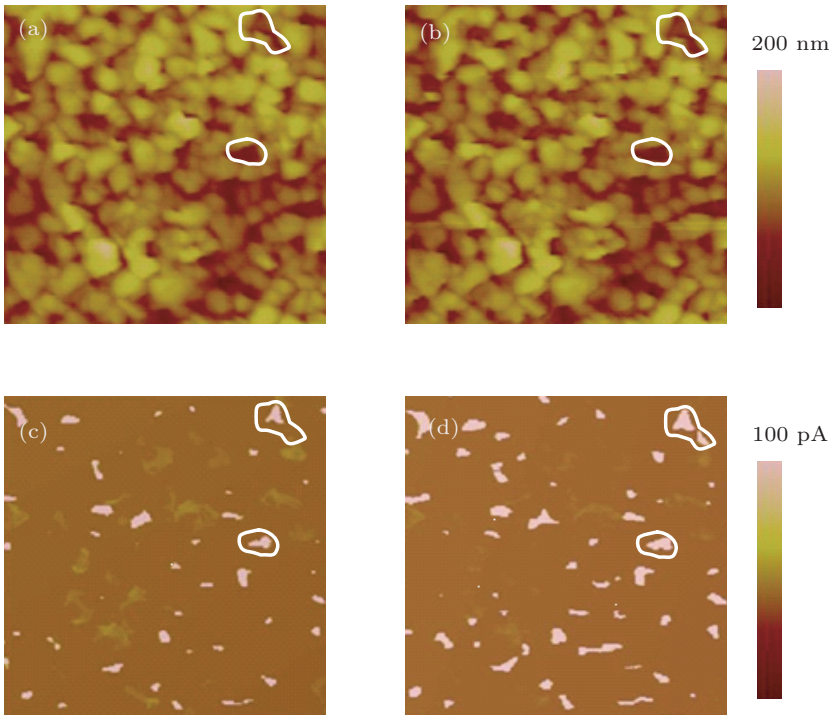

Fig. 6. (colour online) Topography images ((a) and (b)) and corresponding CAFM images in the dark (c) and under the illumination (d). The scanning area is 0.8 μm×0.8 μm.

4. Conclusion

The leakage current behaviours of poly-BFO films are investigated by using both the CAFM and the I–V measurements. From the CAFM images, the local charge transport pathways of the poly-BFO films are found to be located mainly at the grain boundary regions. Furthermore, the leakage current density can be tuned by changing the post-annealing temperature, the annealing time, the bias voltage and the light illumination. These results enable us to control the leakage current behaviours of the BFO films and hence improve the performance of the BFO film-based device.

References

[1] Catalan G and Scott J F 2009 *Adv. Mater.* **21** 2463
[2] Hill N A 2000 *J. Phys. Chem.* B **104** 6694
[3] Wang J, Neaton J B, Zheng H, Nagarajan V, Ogale S B, Liu B, Viehland D, Vaithyanathan V, Schlom D G, Waghmare U V, Spaldin N A, Rabe K M, Wuttig M and Ramesh R 2003 *Science* **299** 1719
[4] Sun Y, Huang Z F, Fan H G, Ming X, Wang C Z and Chen G 2009 *Acta Phys. Sin.* **58** 0193 (in Chinese)
[5] Dho J, Qi X D, Kim H, MacManus-Driscoll J L and Blamire M G 2006 *Adv. Mater.* **18** 1445
[6] Ederer C and Spaldin N A 2005 *Phys. Rev.* B **71** 224103
[7] Singh S K, Ishiwara H, Sato K and Maruyama K 2007 *J. Appl. Phys.* **102** 094109
[8] Kawae T, Terauchi Y, Tsuda H, Kumeda M and Morimoto A 2009 *Appl. Phys. Lett.* **94** 112904
[9] Naganuma H, Miura J and Okamura S 2008 *Appl. Phys. Lett.* **93** 052901
[10] Murari N M, Kumar A, Thomas R and Katiyara R S 2008 *Appl. Phys. Lett.* **92** 132904
[11] Habouti S, Shiva R K, Solterbeck C H, Es-Sounia M and Zaporojtchenko V 2007 *J. Appl. Phys.* **102** 44113
[12] Pabst G W, Martin L W, Chu Y H and Ramesh R 2007 *Appl. Phys. Lett.* **90** 072902
[13] Yang H, Jain M, Suvorova N A, Zhou H, Luo H M, Feldmann D M, Dowden P C, DePaula R F, Foltyn S R and Jia Q X 2007 *Appl. Phys. Lett.* **91** 72911
[14] Xie Z, Luo E Z, Xu J B, Wilson I H, Peng H B, Zhao L H and Zhao B R 2000 *Appl. Phys. Lett.* **76** 1923
[15] Rozier Y, Gautier B, Hyvert G, Descamps A, Plossu C, Dubourdieu C and Ducroquet F 2009 *Thin Soild Films* **517** 1868
[16] Abe K and Komatsu S 1993 *Jpn. J. Appl. Phys.* **32** 4186
[17] Fujisawa H, Shimizu M, Horiuchi T, Shiosaki T and Matsushige K 1997 *Appl. Phys. Lett.* **71** 416
[18] Guillan J, Taravel G, Defay E, Ulmer L, Galera L, Andre B and Baume F 2004 *Integr. Ferroelectr.* **67** 93
[19] Seidel J, Martin L W, He Q, Zhan Q, Chu Y H, Rother A, Hawkridge M E, Maksymovych P, Yu P, Gajek M, Balke N, Kalinin S V, Gemming S, Wang F, Catalan G, Scott J F, Spaldin N A, Orenstein J and Ramesh R 2009 *Nat. Mater.* **8** 229
[20] Hu S H, Hu G J, Meng X J, Wang G S, Sun J L, Guo S L, Chu J H and Dai N 2004 *J. Cryst. Growth* **260** 109

[21] Sushil K S, Shanthy S and Ishiwara H 2010 *J. Appl. Phys.* **108** 054102

[22] Hu H and Krupanidhi S B 1994 *J. Mater. Res.* **9** 1484

[23] Naganuma H, Miura J and Okamura S 2008 *Appl. Phys. Lett.* **93** 52901

[24] Choi T, Lee S, Choi Y J, Kiryukhin V and Cheong S W 2009 *Science* **324** 63

[25] Yang S Y, Martin L W, Byrnes S J, Conry T E, Basu S R, Paran D, Reichertz L, Ihlefeld J, Adamo C, Melville A, Chu Y H, Yang C H, Musfeldt J L, Schlom D G, Ager III J W and Ramesh R 2009 *Appl. Phys. Lett.* **95** 62909

[26] Basu S R, Martin L W, Chu Y H, Gajek M, Ramesh R, Rai R C, Xu X and Musfeldt J L 2008 *Appl. Phys. Lett.* **92** 91905

[27] Qin M, Yao Y and Liang Y C 2008 *Appl. Phys. Lett.* **93** 122904

[28] Luo B C, Chen C L and Xie L 2011 *Acta Phys. Sin.* **60** 027306 (in Chinese)